RSC Advances

PAPER

View Article Online
View Journal | View Issue

Cite this: *RSC Adv.*, 2020, **10**, 27323

Hydrogenation of furfural by noble metal-free nickel modified tungsten carbide catalysts†

Patrick Bretzler,[ab] Michael Huber,[ab] Simon Nickl[ab] and Klaus Köhler[*ab]

Received 2nd March 2020
Accepted 10th July 2020

DOI: 10.1039/d0ra02003f

rsc.li/rsc-advances

Nickel–tungsten carbide catalysts convert furfural to high value products in a liquid phase catalytic reaction. The product distribution depends on the solvent and the Ni–W-ratio of the catalyst. In isopropyl alcohol a combination of Ni and W_xC enables the opening of the furan ring to yield 1,2-pentanediol. Nickel accelerates the tungsten oxide reduction in the tungsten carbide catalyst synthesis and facilitates the carbon insertion. Nickel modified tungsten carbide is a promising, noble metal-free catalyst system for the upgrading of furfural based renewable resources. Its preparation is facilitated compared to unmodified tungsten carbide catalysts.

Introduction

The valorization of renewable resource streams has become one of the most important ways to face declining availability of non-renewable resources. The production of high value chemicals for the chemical industry from biomass instead of petroleum-based resources is becoming increasingly important. Furfural is one of the platform chemicals available from biomass which is suitable for upgrading to high value products.[1,2] Furfural is being produced on an industrial scale by the acidic hydrolysis of pentose sugars, especially arabinose and xylose. The structure of furfural lends itself to the production of several desirable products. Most of the products are formed *via* the intermediate furfuryl alcohol (**FFA**). From there three reaction pathways open up. The hydrodeoxygenation to 2-methylfuran (**2-MF**) and further to 2-methyltetrahydrofuran (**2-MTHF**), the hydrogenation to tetrahydrofurfuryl alcohol (**THFA**) and the ring opening to 1,5-pentanediol (**1,5-PeD**) and 1,2-pentanediol (**1,2-PeD**).[3,4] A simplified network of these reaction products is depicted in Scheme 1. Several other products can be obtained from furfural as well.

1,2-PeD can be used in the production of polyester,[5,6] disinfectants,[6] cosmetics[7] and printing inks.[8] Additionally, **1,2-PeD** possesses interesting properties as an enhancer for the skin permeability of certain drugs.[9,10] The conventional production of **1,2-PeD** from non-renewable petroleum resources is performed in a multistep reaction. Pent-1-ene is oxidized, *e.g.* by the use of H_2O_2, to 1,2-epoxypentane which is further hydrolyzed to **1,2-PeD**.[5,11]

While furfural has moved in to the limelight of research on biomass derived resource streams, only little research has been done on its ring opening to produce pentanediol and the majority of said research focuses on the production of **1,5-PeD**.[12] Most of the catalysts studied for the production of **1,2-PeD** are based on noble metals like Ru,[6] Rh,[13–18] Pd[19,20] and Pt.[3,4,21–23] Most notable are two platinum-based catalysts. Mizugaki *et al.*[4] prepared platinum nanoparticles supported on hydrotalcite and reached a selectivity of 73% to **1,2-PeD**. Koch *et al.*[23] used PtO_2 supported on γ-Al_2O_3 and obtained a selectivity to **1,2-PeD** of up to 80%.

Non-noble metal based catalysts suffer from low yield or limited industrial applicability due to the inherent toxicity of some of the catalysts components, especially Cr and Co. Adkins *et al.*[24,25] prepared the first promising catalysts based on copper chromite already in 1931. More recent works have proposed the use of cobalt based catalysts for the ring opening of furfural.[12,26,27] The product distribution of these catalysts favors **1,5-PeD** over **1,2-PeD** which was only obtained with relatively low yields. The most promising noble metal free catalysts are based on either Ni or Cu. The Ni catalysts typically show a preference to **1,5-PeD**,[28] while copper-based catalysts prepared by Liu *et al.*[29,30] were able to reach a selectivity to **1,2-PeD** of up to 51%.

Tungsten carbide has gained attention as a possible alternative to expensive noble metal hydrogenation catalysts. This interstitial alloy of tungsten and carbon shows similar catalytic properties as platinum in a number of reactions.[31] The low price of tungsten and its widespread availability would make it a desirable catalyst material, if its performance can be tailored to be competitive to more established catalysts. Tungsten carbide has been successfully used in a number of reactions that aim to upgrade biomass-derived resources. Hollak *et al.*[32] studied the deoxygenation of oleic acid. Bitter *et al.*[33–35] converted several fatty acids and guaiacol over tungsten carbide and Guo *et al.*[36] cracked the C–O bonds in lignin feedstock. The

[a]*Department of Chemistry, Inorganic Chemistry, Technical University of Munich, Lichtenbergstrasse 4, 85747 Garching, Germany. E-mail: klaus.koehler@tum.de; Tel: +49 89 289 13233*

[b]*Catalysis Research Center, Technical University of Munich, Ernst-Otto-Fischer-Strasse 1, 85747 Garching, Germany*

† Electronic supplementary information (ESI) available. See DOI: 10.1039/d0ra02003f

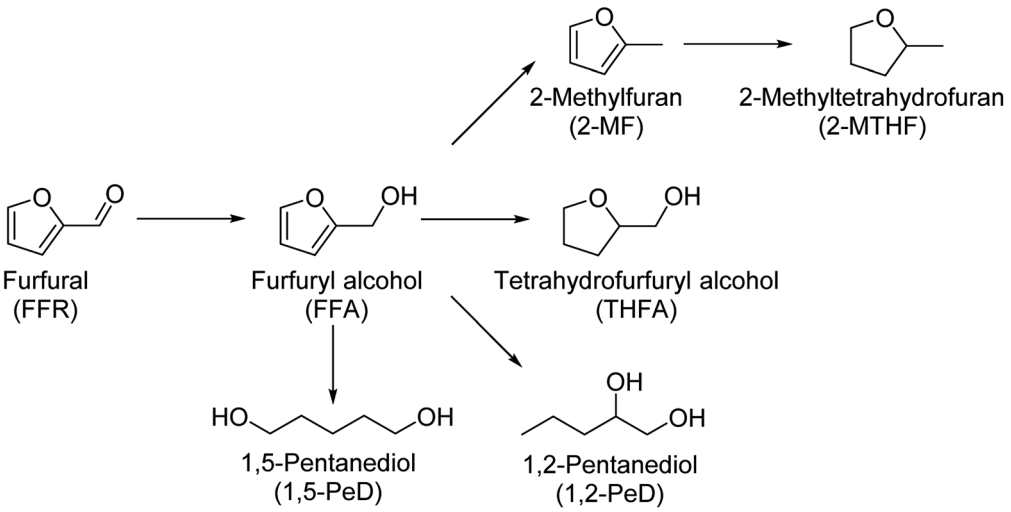

Scheme 1 Reaction network of possible hydrogenation products starting from furfural.[3,4]

activity of tungsten carbide based catalysts can be improved by the addition of nickel. Both cellulose and sugars were successfully converted to ethylene glycol over nickel-modified tungsten carbide catalysts.[37,38]

Huang *et al.*[39] investigated the hydrodeoxygenation of the furfural derivative 5-(hydroxymethyl)furfural to 2,5-dimethylfuran using a Ni-modified tungsten carbide catalyst. In the aprotic solvent tetrahydrofuran (THF) a high yield of 96% could be reached, while no ring opening was observed. The ring-opening to pentanediol is typically performed in protic solvents, like alcohol, or even with the addition of water.[4,40] It stands to reason that a change in solvent could open up different reaction routes and products for the tungsten carbide catalyst system.

The tungsten carbide synthesis is performed at high temperatures, exceeding 700 °C. The carbide catalysts properties are strongly dependent on the synthesis conditions.[41–43] The conversion of tungsten(VI) oxide to tungsten carbide has been studied intensively but the influence of a second metal on this conversion is not fully understood yet. It appears that nickel activates the methane decomposition and facilitates the carbide formation.[44,45] At the same time, any carbon support present in the catalyst precursor is subject to methanation, resulting in extensive sintering.[46]

This work investigates the influence of different Ni-loadings on the isothermal tungsten carbide formation, illuminating the processes that occur during the high temperature carbide synthesis and the crystalline phase composition of the final catalysts. The catalysts are tested for their performance in the hydrogenation of furfural, comparing them to solely W_xC, Ni or $Ni_{17}W_3$ based ones. A special focus is put on the change in product distribution, especially the yield of 1,2-pentanediol, dependent on solvent and Ni–W-ratio.

Experimental

Materials

Chemicals were obtained from Sigma-Aldrich Germany and used without further purification. The chemical's purities are as follows: ammonium metatungstate hydrate 99%, nickel nitrate hexahydrate 99%, furfural 99%, isopropyl alcohol for analysis, 1,4-dioxane 100%. Fumed silica Aerosil 200 was provided by Evonik. The gases are from Westfalen Germany with a purity of ≥99.999% (He, Ar, H_2) or ≥99.5% (CH_4). Argon was used as inert gas in all experiments, except for the temperature-programmed carburization in which He was used.

Precursor

Silica was agglomerated, sieved to a particle size of 100–300 μm, dried at 200 °C for 1 h and calcined at 700 °C for 8 h. The agglomerated silica particles were loaded with 30 mol% (50.0 wt%) tungsten in an incipient wetness impregnation method using a 0.55 M aqueous solution of ammonium metatungstate. This material was dried for 2 h at 60 °C, for 6 h at 110 °C and calcined at 450 °C for 6 h. Ni was loaded on the WO_3/SiO_2 particles in a subsequent or on SiO_2 in a direct incipient wetness impregnation using a nickel nitrate solution. A mixed Ni–W/SiO_2 precursor was obtained in an incipient wetness co-impregnation using a mixed solution of nickel nitrate and ammonium metatungstate in a metal to metal molar ration of 17 : 3 (Ni : W). The impregnation was followed by drying and calcination. Ni-loadings were between 0.5 and 9.0 wt% and 10.0 wt% for NiO/SiO_2. For the Ni–W/SiO_2-precursor the combined metal loading was 10.0 wt%.

Catalyst synthesis and activation

W_xC/SiO_2 and Ni/W_xC/SiO_2 catalysts were synthesized in a horizontal tube furnace under isothermal conditions. The sample was heated under inert gas flow to 700 °C before switching to reactive gas (20% CH_4 in H_2). The effluent gas stream was monitored using a ThermoStar mass spectrometer by Pfeiffer Vacuum. The reduction was determined to be complete once the CO-concentration dropped close to its original value. Afterwards, the catalyst was treated at synthesis

temperature with pure H_2 to remove any excess polymeric carbon from its surface.

Ni/SiO_2 was activated in a horizontal tube furnace by heating to 450 °C under inert gas and reduced under 50% H_2 in Ar for 30 min and 100% H_2 for additional 30 min. $Ni_{17}W_3/SiO_2$ was prepared by heating the sample to 700 °C under inert gas and subsequent reduction in hydrogen. The reduction was deemed complete once the H_2O evolution stopped. All catalysts were cooled under inert gas and transferred to a glove box without contact to air.

XRD

The crystalline phases were examined using an Empyrean X-ray diffractometer by Malvern Panalytical operating with Cu Kα radiation. Samples were measured after passivation in air in reflection geometry in the range from 5–70° 2θ.

BET

The overall surface area of the catalysts was determined by isothermal nitrogen adsorption at −196 °C according to Brunauer–Emmet–Teller on a Quantachrome NovaTouch LX^4. Before the measurement samples were degassed *in vacuo* at 350 °C for 4 h.

Furfural hydrogenation

Catalysis reactions were performed in a 300 mL Parr mini reactor. The reaction mixture consisted of 3 mL furfural, 100 mL isopropyl alcohol and 1.5 mL of 1,4-dioxane as internal standard. The reaction mixture was flushed with Ar before inert addition of 0.50 g catalyst. The reactor was closed and pressurized with H_2 to 65 bar. The reactor was heated to 200 °C before stirring was turned on. Aliquots of the liquid phase where taken through a dip tube several times during the reaction. Samples were analyzed with an Agilent 6980 gas chromatograph from Hewlett Packard equipped with an automated injector and FID. Samples were analyzed over a HP-1 MS column with the following temperature-program – holding at 50 °C for 3 min and heating to 270 °C with 30 K min^{-1}. Retention times and response factors relative to the internal standard were determined using pure substances. The conversion and yield are calculated according to equations in the ESI.†

Results and discussion

Synthesis of Ni-modified tungsten carbide catalysts and the role of nickel in the W_xC synthesis

For tungsten carbide catalysts, the processes occurring during the carbide synthesis and in turn the properties of the final catalyst are highly dependent on the synthesis conditions. The addition of nickel is a substantial interference on the synthesis of the carbide-catalyst. Therefore, the reduction and carbon insertion occurring during the synthesis is explored in the first subsection. Silica is added to the catalyst to provide a non-reducible support and to stabilize a high tungsten carbide surface area.

Preparation of Ni-modified tungsten oxide–silica precursors. The $NiO/WO_3/SiO_2$ precursor is prepared in a sequential incipient wetness impregnation. The agglomerated silica parent particles are loaded with 50.0 wt% tungsten in a first impregnation–calcination process. In a second incipient wetness impregnation, between 0.5–9.0 wt% nickel is loaded on to this WO_3/SiO_2 precursor. The material is calcined to form $NiO/WO_3/SiO_2$ with nickel preferably deposited on the surface of the particles. The catalyst precursor is then subjected to an isothermal carbide synthesis. The processes occurring during this high temperature synthesis reaction and the role nickel plays in it are discussed in the following section.

Isothermal tungsten carbide synthesis. In the isothermal tungsten carbide synthesis the precursor is heated in an inert gas and only after reaching 700 °C is it exposed to the reactive gas mixture (20% CH_4 in H_2). This results in the reduction and carburization steps proceeding either simultaneously or consecutively, but not separated by their onset temperature. The reduction and carburization of WO_3 results in the formation of H_2O and CO. The CO formation is not directly connected to the insertion of carbon into tungsten but can be seen as an indication of CH_4-activation. The CO-concentration in the effluent gas stream during the isothermal synthesis is depicted in Fig. 1.

Without Ni the CO-evolution at 700 °C only starts after an initiation period of 25 min. The CO-concentration in the effluent gas stream slowly increases before gradually declining after passing through a maximum after 100 min and dropping back to the baseline after 130 min. The end of the CO-formation indicates the completion of the reduction and possibly the carbon insertion.

The addition of Ni cuts the duration of the initiation period in half and results in a steep increase of the CO-concentration in the exhaust gas stream. The CO-formation quickly passes through a maximum and gradually declines again. The CO-signal reaches the baseline typically after 75 min. The addition of Ni halves the time needed to complete the reduction, with only little influence of the total Ni-loading on this behavior. Only for the lowest Ni-loading of 0.5 wt% is this behavior slightly different. Here the CO-evolution is split into two maxima, a first one at 11 min and a second one at 28 min. Additionally, the complete reduction time is slightly longer with 95 min compared to 70 min for all higher Ni-loadings. The initiation period is shorter for low Ni-loadings and becomes longer when more Ni is added. It is possible that Ni has to be completely reduced to its metallic state before it can activate CH_4, resulting in CO-formation. This Ni reduction takes more time when a larger amount of Ni is present.

The overall surface area of the catalysts, as measured by BET, gradually decreases from 97 $m^2 g^{-1}$ for no addition of Ni to 70 $m^2 g^{-1}$ for the addition of 10 wt% Ni. More details are shown in Table S1.† Some of this loss in surface area can be attributed to the second calcination step during the catalyst preparation when Ni is added. A second effect is likely the blocking of pores with increasing nickel loadings.

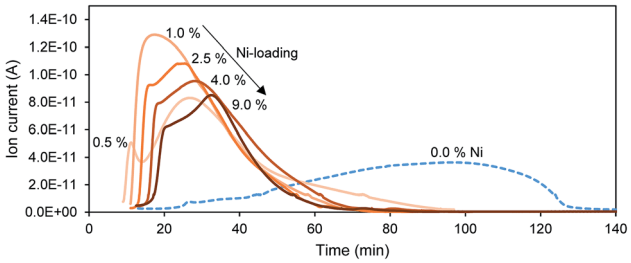

Fig. 1 CO in the effluent gas stream during isothermal W_xC synthesis in a horizontal tube furnace at 700 °C in reactive gas (20% CH_4 in H_2). The reaction is starting from WO_3/SiO_2 with different mass-loadings of Ni; no Ni: blue, dashed line; increasing amounts of Ni: darker shades of orange, solid lines.

Crystalline phase composition. Adding nickel to the precursor changes the ratios of the crystalline phases of the final catalyst (Fig. 2). Without the addition of Ni mostly W_2C is formed, containing only small amounts of metallic W. The presence of silica in the precursor stabilizes the metastable W_2C and limits the formation of the thermodynamically favored WC. Adding 0.5 wt% Ni to the WO_3/SiO_2-precursor results in the complete disappearance of the reflexes of metallic tungsten at 41° and 58°. The only remaining reflexes are those of W_2C. The reflexes of WC at 31°, 35°, 48° and less prominently at 64° and 65° only appear after the addition of nickel. Further increasing the amount of Ni increases the amount of WC found in the catalyst. Nickel itself forms an alloy with tungsten and is present as $Ni_{17}W_3$, with reflexes visible at 44° and 51° for Ni-loadings of 2.5 wt% and above. In the presence of Ni the carbon insertion proceeds more complete, resulting in a greater amount of WC instead of W_2C and W. The Ni- and $Ni_{17}W_3$-catalysts only show the reflexes of the respective metallic phases (ESI Fig. S1†).

In summary, the addition of nickel to the WO_3/SiO_2 precursor alters the carbide formation in several ways. Nickel activates hydrogen and methane, resulting in altered reduction steps. Methane plays a more dominant role during the reduction. The isothermal reduction is substantially faster, even for the addition of only a small amount of nickel. The carbon insertion is assisted and the composition of the crystalline phases changes towards a higher amount of WC. Nickel itself forms a $Ni_{17}W_3$-alloy with tungsten. The synthesis of tungsten carbide catalysts is facilitated, forming the carbide more readily.

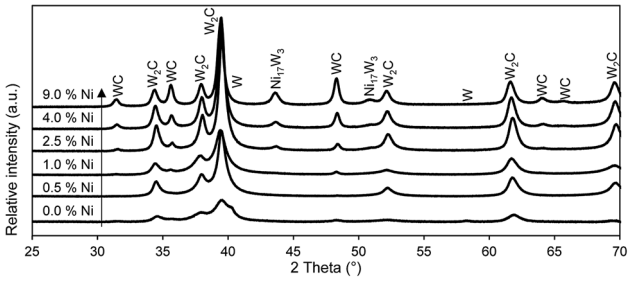

Fig. 2 X-ray diffractograms of tungsten carbide catalysts with different Ni-loadings. The Ni-loading is indicated as weight% of the WO_3/SiO_2 precursor. Catalysts are prepared in an isothermal reaction at 700 °C. Reference patterns from ICDD database, WC: 00-025-1047,[47] W_2C: 00-35-0776,[48] W: 00-001-1203 [49] and $Ni_{17}W_3$: 03-065-4828.[50]

Catalytic conversion of furfural over Ni-modified tungsten carbide catalysts

The carbide synthesis resulted in tungsten carbide catalysts with Ni-loadings from 0.0 wt% to 9.0 wt%. These catalysts are investigated for the hydrogenation of furfural at 200 °C under 65 bar H_2-pressure. The catalytic activity and the product distribution are the focus of this work. Both aspects are heavily influenced by the solvent and the Ni-loading, which are at the center of the next subsections.

Influence of the solvent on product distribution. The nature of the solvent has an immense influence on the conversion rate and the formed products. In the aprotic solvent THF, the reaction proceeds *via* the hydrodeoxygenation of furfuryl alcohol to 2-methylfuran. The furfural is only consumed after a reaction time of 6 h and intermediary furfuryl alcohol can still be detected after this time. Only a small amount of the reaction product 2-methylfuran is further hydrogenated to 2-methyltetrahydrofurane. In THF the reaction proceeds with moderate conversion rates selectively *via* the hydrodeoxygenation pathway as shown in Fig. 3a. These results are in accordance with the results reported by Fu *et al.*[39] on the hydrodeoxygenation of 5-(hydroxymethyl)furfural by a nickel–tungsten carbide catalyst on activated carbon.

Using isopropyl alcohol as a solvent results in a different product distribution and overall faster conversion of furfural. The reaction starts from furfural over furfuryl alcohol, where three competing reaction pathways open up. Furfural is hydrogenated much faster than in THF, with complete conversion to furfuryl alcohol after only 15 min instead of after 6 h. This secondary product is converted much faster too. All furfuryl alcohol is reacted after 90 min. Initially a mixture of three reaction products is formed: 2-methylfuran (**2-MF**), which is further hydrogenated to 2-methyltetrahydrofuran (**2-MTHF**), tetrahydrofurfuryl alcohol (**THFA**), and 1,2-pentanediol (**1,2-PeD**). In isopropyl alcohol, the alcohol functionality can be preserved to some extent and the opening of the furan ring is possible (Fig. 3b). The amount of unidentified products is similarly high for both solvents, with 23.8% for THF and 21.9% for isopropyl alcohol.

The two solvents differ in their polarity, their ability to form adducts with the reactants and intermediary products, and their hydrogen solubility. Isopropyl alcohol can form an acetal with furfural and ethers with all alcohol group bearing intermediary products. Together with the higher polarity of the protic solvent, this results in a preferential transformation to alcohol group containing products. The hydrogen solubility is much higher in isopropyl alcohol,[51,52] explaining the lower reaction rate and incomplete hydrogenation of **2-MF** in THF.

Influence of the Ni–W-ratio on the furfural hydrogenation. The ratio of Ni and W_xC and the interplay of these two catalyst

components has a strong influence on the product formation and catalytic performance of these materials. While only the overall results of the catalysis test are discussed here, the reaction progress for catalysts with different Ni–W ratios can be found in the ESI.†

Rate of furfural conversion. The catalysts activity for the conversion of furfural is highly dependent on the Ni-loading. For catalysts with high Ni-loadings, the reactant furfural is quickly converted to the intermediary product furfuryl alcohol. Measuring the exact time needed until full furfural conversion is reached is imprecise due to this fast reaction rate. To achieve more reliable information about the catalysts activity, the time needed for the complete conversion of the secondary product furfuryl alcohol is used. This time is defined as the first sampling, where the sample does not contain furfuryl alcohol, giving a good indication of the catalyst's activity.

Unmodified tungsten carbide catalysts show poor catalytic activity and only reach full conversion after 14–24 h at 200 °C. Pure nickel catalysts on the other hand possess a very high catalytic activity, converting all furfuryl alcohol in only 30 min. Nickel modified tungsten carbide catalysts fall in between those two extremes, depending on their Ni-loading. A low Ni-loading of 0.5 wt% significantly improves the catalytic activity but still not all furfuryl alcohol is converted after 6 h. Further increasing the Ni-loading lowers the time until full conversion is reached, approaching the activity of pure Ni-catalysts at high Ni-loadings as shown in Fig. 4. The use of W_xC does not improve the conversion rate compared to catalysts solely based on Ni but in the Ni-W_xC-system activity can be traded for a change in product distribution, as will be shown in the next subsection.

Product distribution. The formed products vary greatly depending on the Ni/W-ratio when using the same solvent (isopropyl alcohol) and reaction conditions (200 °C, 65 bar H_2, Table 1). Tungsten carbide without the addition of Ni results mostly in the formation of **2-MF** with no further hydrogenation to **2-MTHF**. Ni on silica without tungsten carbide yields different products. The higher hydrogenation activity results in the formation of fully saturated **2-MTHF** instead of **2-MF**. Furthermore, the hydrodeoxygenation is no longer the dominant pathway and the main product becomes **THFA**.

Modifying the tungsten carbide catalyst with Ni changes the product distribution towards that of the Ni/SiO_2-catalyst. The products of the hydrodeoxygenation pathway are more thoroughly hydrogenated to **2-MTHF** with a decreasing total amount of substance following this pathway. **THFA** becomes more prevalent with increasing amounts of nickel. This change from the tungsten carbide to the nickel based system is very gradual and follows the changing ratio of Ni and W.

Interestingly, for medium Ni-loadings the ring opening of furfuryl alcohol to **1,2-PeD** is observed. This product only appears for catalysts with a combination of nickel and tungsten carbide. The highest selectivity of 21% is obtained for 2.5 wt% Ni with a lower selectivity at either lower or higher Ni-loadings. The addition of W to Ni and the formation of $Ni_{17}W_3$ alone does only results in very miniscule amounts of this ring-opening product.

The combination of $Ni_{17}W_3$ and W_xC gives rise to a different reaction pathway, which allows the opening of the furan ring while keeping both oxygen functionalities of the molecule. This reaction appears to be dependent on the simultaneous presence of tungsten carbide and nickel. The catalytic behavior of both tungsten carbide and nickel, for either the hydrodeoxygenation route or the formation of **THFA**, are mostly unaffected by this additional reactivity.

Reusability of the catalyst. The catalyst's reusability is tested by adding additional furfural after a first catalysis test. For this addition, the reactor is cooled down and depressurized. Furfural is added together with solvent to make up for the volume lost during sampling in the first catalysis test. The reaction mixture of the first test is not removed to avoid the loss of catalyst material and exposure to air. The reactivation of tungsten carbide catalysts is difficult once they are exposed to air.[53]

The furfural conversion is slower in the second catalytic run. Furfural is only consumed after 2 h instead of after 45 min. The

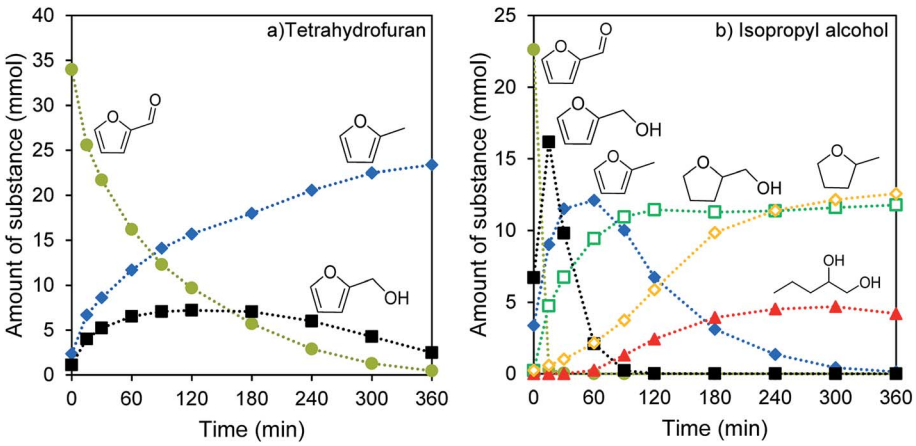

Fig. 3 Reaction progress during the catalytic conversion of furfural in (a) tetrahydrofuran and (b) isopropyl alcohol as solvent. The reaction proceeds at 200 °C under 65 bar H_2, with 0.50 g 4%-Ni/W_xC/SiO_2 and 3 mL furfural.

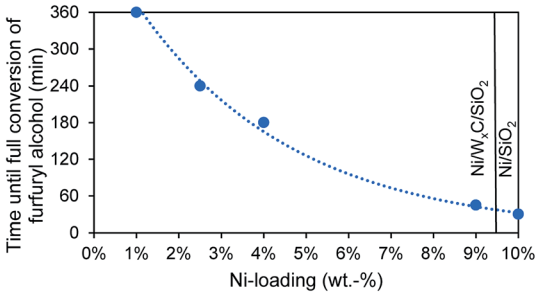

Fig. 4 Time needed until full conversion of the intermediary product furfuryl alcohol for catalysts with different Ni-loadings. The catalyst with 10 wt% Ni consists only of Ni without a tungsten component. The reaction proceeds at 200 °C, 65 bar H_2 with 0.50 g catalyst and 3 mL furfural in isopropyl alcohol as solvent.

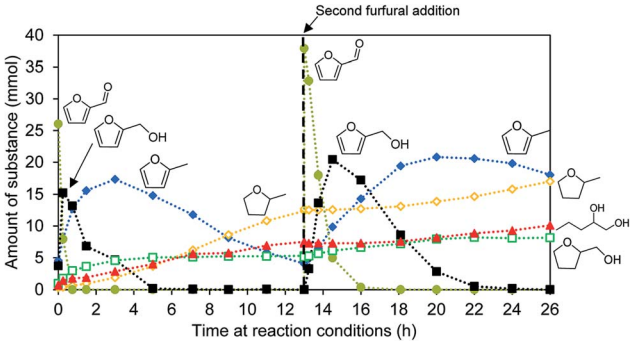

Fig. 5 Reaction progress during catalytic conversion of furfural with 2.5 wt% Ni/W_xC/SiO_2. The reaction proceeds at 200 °C under 65 bar H_2, with 0.5 g catalyst in isopropyl alcohol as solvent. Initially 3 mL furfural are added and after 13 h of reaction time the reactor is cooled down and depressurized to add further 3 mL of furfural before continuing the reaction.

intermediary furfuryl alcohol can be detected for 11 h instead of 5 h. The time needed until full conversion is doubled during the second catalysis test run (Fig. 5).

Not only the conversion rate changes, but the product distribution is modified as well (Table 2). The hydrodeoxygenation pathway is still prominent but the hydrogenation of the unsaturated bonds in the furan ring is hindered, resulting in more **2-MF**. The hydrogenation of the double bonds and the ring opening without loss of the oxygen functionality is inhibited, producing less **THFA** and **1,2-PeD**. The amount of unidentified products increases from 26.1% to 36.4%.

The catalyst undergoes changes during the first catalysis run or the addition of the new substrate. These changes have an effect on the product distribution and conversion rate of the second run. It appears that several different active centers are available on the catalyst, which deactivate to a varying extent. The hydrodeoxygenation is less affected than the hydrogenation and ring opening. The reactions that are catalyzed by the Ni-component are more affected than the ones catalyzed by W_xC. The X-ray diffraction pattern does not change during the catalysis test (Fig. S2†), therefore it is unlikely that one active component is lost during the reaction. A possible mechanism for this deactivation is the deposition of polymerized furfural derivatives and coke precursors blocking certain active sites.

Hypothesis on the nature of the active site for the 1,2-pentanediol formation

As the ring opening of furfural to produce 1,2-pentanediol belongs to the most interesting findings of this work, the possible nature of the active site responsible for this reaction is further discussed. The results obtained in this work can only give a first idea of a possible mechanism but to conclusively uncover the exact working of this catalyst more work will be needed. Only the mixture of nickel and tungsten carbide gives rise to the formation of 1,2-pentanediol. This valuable reaction product is obtained neither over tungsten carbide, nor over nickel catalysts on their own. The combination of the active materials $Ni_{17}W_3$ and W_xC appears to enable the ring opening and the formation of this reaction product.

Since the material is preferentially formed on a certain mixture of nickel and tungsten carbide, it can be expected that the active sites for the ring opening rely on a combination of both materials. The critical step for the determination of the product distribution is the reaction of the intermediary product

Table 1 Product yield for different catalysts after furfural hydrogenation at 200 °C under 65 bar H_2 with 0.50 g catalyst in isopropyl alcohol as solvent. The reaction time is 6 h except for the catalyst without Ni addition, where it is 24 h. Full conversion of furfural is reached in all cases

			Yield%				
			Hydrodeoxygenation		Hydrogenation	Ring opening	
Entry	Catalyst	Reaction time (h)	**2-MF**	**2-MTHF**	**THFA**	**1,2-PeD**	**1,5-PeD**
1	W_xC/SiO_2	24	45	—	—	—	13
2	0.5%-Ni/W_xC/SiO_2	6	36	1	4	3	—
3	1.0%-Ni/W_xC/SiO_2	6	26	15	14	9	—
4	2.5%-Ni/W_xC/SiO_2	6	11	25	20	21	—
5	4.0%-Ni/W_xC/SiO_2	6	—	35	32	12	—
6	9.0%-Ni/W_xC/SiO_2	6	1	36	45	4	—
7	10.0%-Ni/SiO_2	6	—	29	46	—	—
8	10.0%-$Ni_{17}W_3/SiO_2$	6	10	39	35	2	—

Table 2 Product distribution for 2.5%-Ni/W_xC/SiO_2 after 13 h reaction time at 200 °C under 65 bar H_2 for two consecutive catalysis runs. The product distribution is separate for each furfural addition. The reaction vessel was cooled down and depressurized before the second addition of furfural. Full furfural conversion was reached in both cases

		Yield%				
		Hydrodeoxygenation		Hydrogenation	Ring opening	
Entry	Run	**2-MF**	**2-MTHF**	**THFA**	**1,2-PeD**	**1,5-PeD**
1	First	10.2	31.3	13.4	19.0	—
2	Second	31.1	15.4	7.9	9.2	—

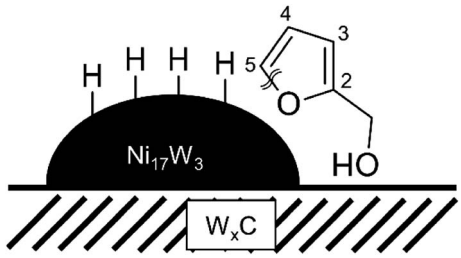

Scheme 2 Possible orientation of furfuryl alcohol at the proposed active site for the ring opening, the boundary between $Ni_{17}W_3$ and W_xC. Based on the proposed reaction path by Mizugaki *et al.*[4]

furfuryl alcohol. Mizugaki *et al.*[4] provided a possible reaction pathway of furfuryl alcohol to 1,2-pentanediol over Pt-nanoparticles supported on hydrotalcite, which places the active site at the boundary between platinum and support. In their proposed reaction pathway the alcohol group of **FFA** interacts with the basic surface sites of the hydrotalcite, orienting the furan ring towards the Pt-particle. The platinum then provides activated hydrogen and enables the ring opening at the C–O bond pointing away from the alcohol group.

A very similar reaction mechanism could be possible for Ni supported on W_xC. In this case, the oxophilic tungsten carbide could attract the oxygen of the alcohol group and orient the furan ring towards the nickel-particle. The nickel then enables the actual ring opening. Scheme 2 depicts this process. Following this hypothetical reaction mechanism places the active site for the ring opening of furfural right at the boundary between W_xC and Ni.

The reaction pathways occurring on solely Ni and W_xC still dominate the overall product distribution for the tested catalysts. By improving the amount of active sites for the ring opening, the selectivity to 1,2-pentanediol could possibly be improved. At the same time, it might be possible to suppress selectively the hydrodeoxygenation and hydrogenation without ring opening by optimization of the synthesis conditions or a targeted deactivation of certain active sites. Investigations to improve the catalyst in this manner are already in progress.

Conclusion

The high temperature formation of the potential platinum substitute W_xC is strongly influenced by the presence of Ni in the WO_3-precursor. The added Ni activates the CH_4 and H_2 used in the carbide synthesis, facilitating the tungsten oxide reduction and carbon insertion. The time needed for complete reduction of WO_3 is cut in half and the carbon insertion proceeds more completely, resulting in more WC and less W_2C and W.

The Ni–W-ratio and nature of the solvent play a crucial role in the formation of the high-value reaction product 1,2-pentanediol from furfural. No ring-opening occurs in THF, while in isopropyl alcohol, 1,2-pentanediol is formed.

The rate of conversion of furfural and furfuryl alcohol is strongly dependent on the Ni–W-ratio in the catalyst, with higher rates being achieved for high Ni-loadings. The combination of Ni and W_xC gives rise to the formation of 1,2-pentanediol, which is fformed on neither a solely W_xC- nor a Ni-based catalyst. By controlling the Ni–W-ratio the product distribution can be tailored to increase the yield of 1,2-pentanediol.

Future work must be focused to improve the selectivity and stability of the Ni/W_xC-catalyst system. Nickel modified tungsten carbides provide a hopeful starting point for the development of non-noble metal catalysts for the upgrading of biomass derived furfural. Both problems of selectivity and stability can possibly be tackled by optimizing the precursor and tungsten carbide syntheses.

Conflicts of interest

There are no conflicts to declare.

Acknowledgements

P. B. thanks the TUM Graduate School for financial support. We want to thank Hannah Augenstein for providing a nickel on silica catalyst.

References

1 N. S. Biradar, A. M. Hengne, S. N. Birajdar, P. S. Niphadkar, P. N. Joshi and C. V. Rode, *ACS Sustainable Chem. Eng.*, 2014, **2**, 272–281.
2 K. Yan, G. Wu, T. Lafleur and C. Jarvis, *Renewable Sustainable Energy Rev.*, 2014, **38**, 663–676.
3 W. Xu, H. Wang, X. Liu, J. Ren, Y. Wang and G. Lu, *Chem. Commun.*, 2011, **47**, 3924.

4 T. Mizugaki, T. Yamakawa, Y. Nagatsu, Z. Maeno, T. Mitsudome, K. Jitsukawa and K. Kaneda, *ACS Sustainable Chem. Eng.*, 2014, **2**, 2243–2247.
5 R. Siegmeier, G. Prescher and H. Maurer, European Pat., 0,257,243, 1987.
6 B. Zhang, Y. Zhu, G. Ding, H. Zheng and Y. Li, *Green Chem.*, 2012, **14**, 3402–3409.
7 I. Agostini and S. Cupferman, *US Pat.*, US 6,296,858 B1, 2001.
8 K. Aoki and H. Mukai, Japan Pat., JP2012245721, 2012.
9 L. Duracher, L. Blasco, J.-C. Hubaud, L. Vian and G. Marti-Mestres, *Int. J. Pharm.*, 2009, **374**, 39–45.
10 N. Li, W. Jia, Y. Zhang, M. C. Zhang, F. Tan and J. Zhang, *AAPS PharmSciTech*, 2014, **15**, 354–363.
11 R. Siegmeier, G. Prescher, H. Maurer and G. Hering, *US Pat.*, 4,605,795, 1986.
12 T. P. Sulmonetti, B. Hu, S. Lee, P. K. Agrawal and C. W. Jones, *ACS Sustainable Chem. Eng.*, 2017, **5**, 8959–8969.
13 S. Liu, Y. Amada, M. Tamura, Y. Nakagawa and K. Tomishige, *Catal. Sci. Technol.*, 2014, **4**, 2535–2549.
14 M. Chia, Y. J. Pagan-Torres, D. Hibbitts, Q. Tan, H. N. Pham, A. K. Datye, M. Neurock, R. J. Davis and J. A. Dumesic, *J. Am. Chem. Soc.*, 2011, **133**, 12675–12689.
15 J. Guan, G. Peng, Q. Cao and X. Mu, *J. Phys. Chem. C*, 2014, **118**, 25555–25566.
16 S. Koso, I. Furikado, A. Shimao, T. Miyazawa, K. Kunimori and K. Tomishige, *Chem. Commun.*, 2009, 2035–2037.
17 M. Chatterjee, H. Kawanami, T. Ishizaka, M. Sato, T. Suzuki and A. Suzuki, *Catal. Sci. Technol.*, 2011, **1**, 1466–1471.
18 D. S. Pisal and G. D. Yadav, *ACS Omega*, 2019, **4**, 1201–1214.
19 S. Liu, Y. Amada, M. Tamura, Y. Nakagawa and K. Tomishige, *Green Chem.*, 2014, **16**, 617–626.
20 N. S. Date, R. C. Chikate, H.-S. Roh and C. V. Rode, *Catal. Today*, 2018, **309**, 195–201.
21 W. E. Kaufmann and R. Adams, *J. Am. Chem. Soc.*, 1923, **45**, 3029–3044.
22 T. Tong, X. Liu, Y. Guo, M. Norouzi Banis, Y. Hu and Y. Wang, *J. Catal.*, 2018, **365**, 420–428.
23 O. Koch, A. Köckritz, M. Kant, A. Martin, A. Schöning, U. Armbruster, M. Bartoszek, S. Evert, B. Lange and R. Bienert, *US Pat.*, US2014/0066666A1, 2014.
24 H. Adkins and R. Connor, *J. Am. Chem. Soc.*, 1931, **53**, 1091–1095.
25 R. Connor and H. Adkins, *J. Am. Chem. Soc.*, 1932, **54**, 4678–4690.
26 F. Gao, H. Liu, X. Hu, J. Chen, Z. Huang and C. Xia, *Chin. J. Catal.*, 2018, **39**, 1711–1723.
27 J. Lee, S. P. Burt, C. A. Carrero, A. C. Alba-Rubio, I. Ro, B. J. O'Neill, H. J. Kim, D. H. K. Jackson, T. F. Kuech, I. Hermans, J. A. Dumesic and G. W. Huber, *J. Catal.*, 2015, **330**, 19–27.
28 H. W. Wijaya, T. Kojima, T. Hara, N. Ichikuni and S. Shimazu, *ChemCatChem*, 2017, **9**, 2869–2874.
29 H. Liu, Z. Huang, H. Kang, C. Xia and J. Chen, *Chin. J. Catal.*, 2016, **37**, 700–710.
30 H. Liu, Z. Huang, F. Zhao, F. Cui, X. Li, C. Xia and J. Chen, *Catal. Sci. Technol.*, 2016, **6**, 668–671.
31 R. B. Levy and M. Boudart, *Science*, 1973, **181**, 547–549.
32 S. A. W. Hollak, R. W. Gosselink, D. S. van Es and J. H. Bitter, *ACS Catal.*, 2013, **3**, 2837–2844.
33 R. W. Gosselink, D. R. Stellwagen and J. H. Bitter, *Angew. Chem., Int. Ed.*, 2013, **52**, 5089–5092.
34 D. R. Stellwagen and J. H. Bitter, *Green Chem.*, 2015, **17**, 582–593.
35 A. L. Jongerius, R. W. Gosselink, J. Dijkstra, J. H. Bitter, P. C. A. Bruijnincx and B. M. Weckhuysen, *ChemCatChem*, 2013, **5**, 2964–2972.
36 H. Guo, B. Zhang, C. Li, C. Peng, T. Dai, H. Xie, A. Wang and T. Zhang, *ChemSusChem*, 2016, **9**, 3220–3229.
37 A. Wang and T. Zhang, *Acc. Chem. Res.*, 2013, **46**, 1377–1386.
38 R. Ooms, M. Dusselier, J. A. Geboers, B. Op de Beeck, R. Verhaeven, E. Gobechiya, J. A. Martens, A. Redl and B. F. Sels, *Green Chem.*, 2014, **16**, 695–707.
39 Y.-B. Huang, M.-Y. Chen, L. Yan, Q.-X. Guo and Y. Fu, *ChemSusChem*, 2014, **7**, 1068–1072.
40 R. Ma, X.-P. Wu, T. Tong, Z.-J. Shao, Y. Wang, X. Liu, Q. Xia and X.-Q. Gong, *ACS Catal.*, 2017, **7**, 333–337.
41 G. Leclercq, M. Kamal, J. M. Giraudon, P. Devassine, L. Feigenbaum, L. Leclercq, A. Frennet, J. M. Bastin, A. Löfberg, S. Decker and M. Dufour, *J. Catal.*, 1996, **159**, 142–169.
42 A. Löfberg, A. Frennet, G. Leclercq, L. Leclercq and J. M. Giraudon, *J. Catal.*, 2000, **189**, 170–183.
43 T. Xiao, A. Hanif, A. P. E. York, J. Sloan and M. L. H. Green, *Phys. Chem. Chem. Phys.*, 2002, **4**, 3522–3529.
44 N. Ji, T. Zhang, M. Zheng, A. Wang, H. Wang, X. Wang, Y. Shu, A. L. Stottlemyer and J. G. Chen, *Catal. Today*, 2009, **147**, 77–85.
45 N. Ji, T. Zhang, M. Zheng, A. Wang, H. Wang, X. Wang and J. G. Chen, *Angew. Chem., Int. Ed.*, 2008, **47**, 8510–8513.
46 N. Ji, M. Zheng, A. Wang, T. Zhang and J. G. Chen, *ChemSusChem*, 2012, **5**, 939–944.
47 L. N. Butorina, *Sov. Phys. Crystallogr.*, 1960, **5**, 216.
48 E. Rudy and S. Windisch, *J. Am. Ceram. Soc.*, 1967, **50**, 272.
49 W. P. Davey, *Phys. Rev.*, 1925, **25**, 753–761.
50 F. Abe and T. Tanabe, *Z. Metallkd.*, 1985, **76**, 420.
51 E. Brunner, *Berichte der Bunsengesellschaft für physikalische Chemie*, 1979, **83**, 715–721.
52 E. Brunner, *J. Chem. Eng. Data*, 1985, **30**, 269–273.
53 A. Mehdad, R. E. Jentoft and F. C. Jentoft, *J. Catal.*, 2017, **347**, 89–101.

